Supporting Information (SI) for

Highly Sensitive Bifunctional Probe for Colorimetric Cyanide and Fluorometric H_2S Detection and Bioimaging: Spontaneous Resolution, Aggregation and Multicolor Fluorescence of Bisulfide Adduct

Sumit Kumar Patra,[†] Sanjoy Kumar Sheet,[†] Bhaskar Sen,[†] Kripamoy Aguan,[‡] Debesh Ranjan Roy,[§] and Snehadrinarayan Khatua*[†]

[†]Centre for Advanced Studies, Department of Chemistry, North Eastern Hill University, Shillong, Meghalaya 793022, India.

[‡]Department of Biotechnology and Bioinformatics, North Eastern Hill University, Shillong, Meghalaya 793022, India.

[§]Applied Physics Department, S.V. National Institute of Technology, Surat 395 007, India

Table of Contents **Page no**

1	Characterization Checklist and list of compounds	S2
2	NMR spectra of **MBA**	S3
3	ESI-MS spectra of **MBA**	S4
4	NMR spectra of **1**	S4-S5
5	ESI-MS spectra of **1**	S5
6	Absorbance change upon addition of cyanide (0-1.5 equiv)	S6
7	Interference Studies in UV-vis channel	S6
8	ESI-MS of 1+ Cyanide	S7
9	Computational studies	S7-S9
10	Absorption titration of **1** with H_2S	S10
11	Fluorescence response of probe **1** with Cys and GSH	S10
12	Fluorescence changes upon addition of H_2S (0-1.4 equiv.)	S11
13	Calculation of Detection limit in fluorescence channel	S11
14	Interference Studies in fluorescence channel	S12
15	Effect of pH in fluorescence channel	S12
16	ESI-MS and ^{1}H NMR spectra of **1-SH** adduct	S13
17	HPLC analysis	S14
18	Fluorescence of **1-SH** in solvents of different polarities	S15
19	UV-vis spectra of **1-SH** in different concentration	S15
20	Cytotoxicity studies	S16
21	ORTEP plot of probe **1** and **1-SH** adduct	S17
22	Crystal data and structure refinement for **1** and **1-SH**	S18

Techniques		Compounds		
		MBA	**1**	**1-SH**
Elemental analysis		✓	✓	-
ESI-MS spectrometry		✓	✓	✓
FTIR spectroscopy		✓	✓	-
1D NMR Spectroscopy	^{1}H	✓	✓	✓
	^{13}C	✓	✓	-
Single crystal X-ray diffraction		-	✓	✓
UV-vis spectroscopy		-	✓	✓
Fluorescence spectroscopy		-	✓	✓
HPLC		-	✓	✓

List of Compounds:

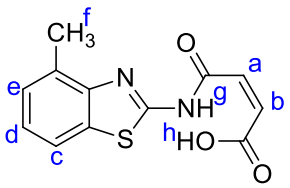

MBA

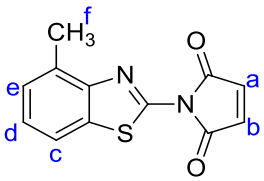

1

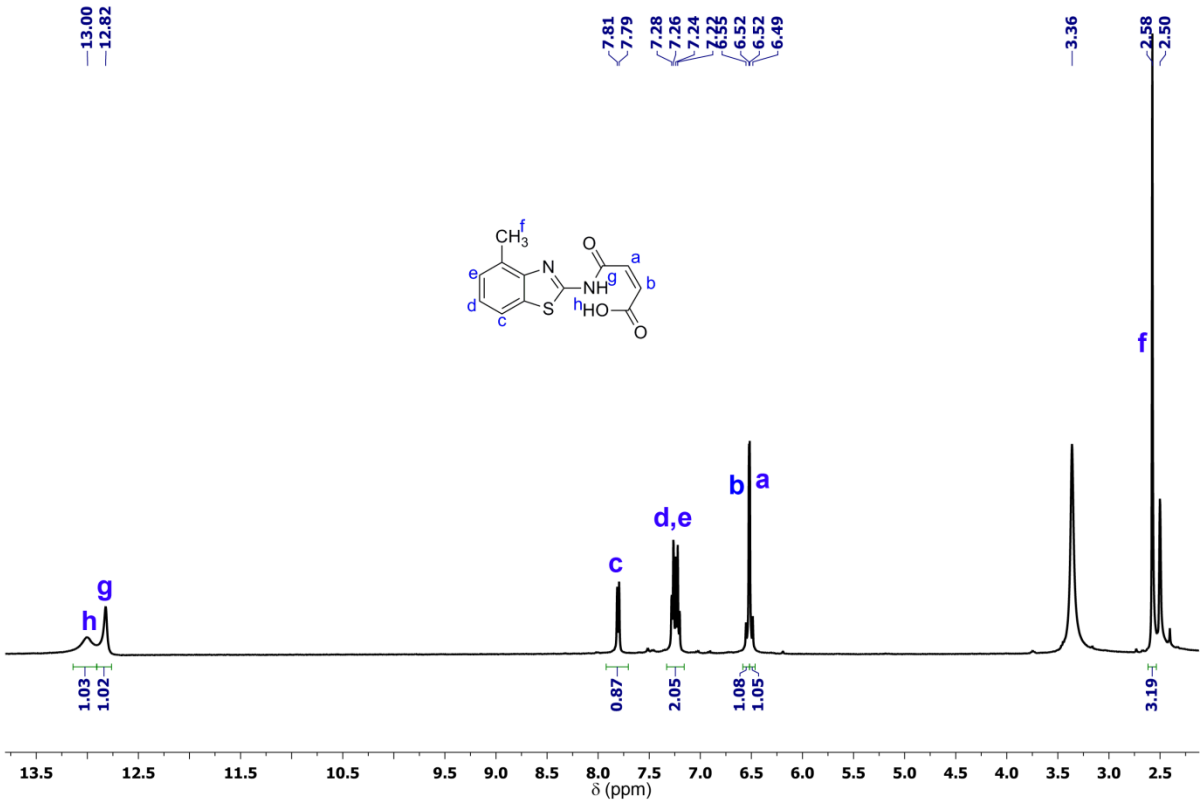

Figure S1. ^{1}H NMR spectrum of **MBA** in DMSO-d_6.

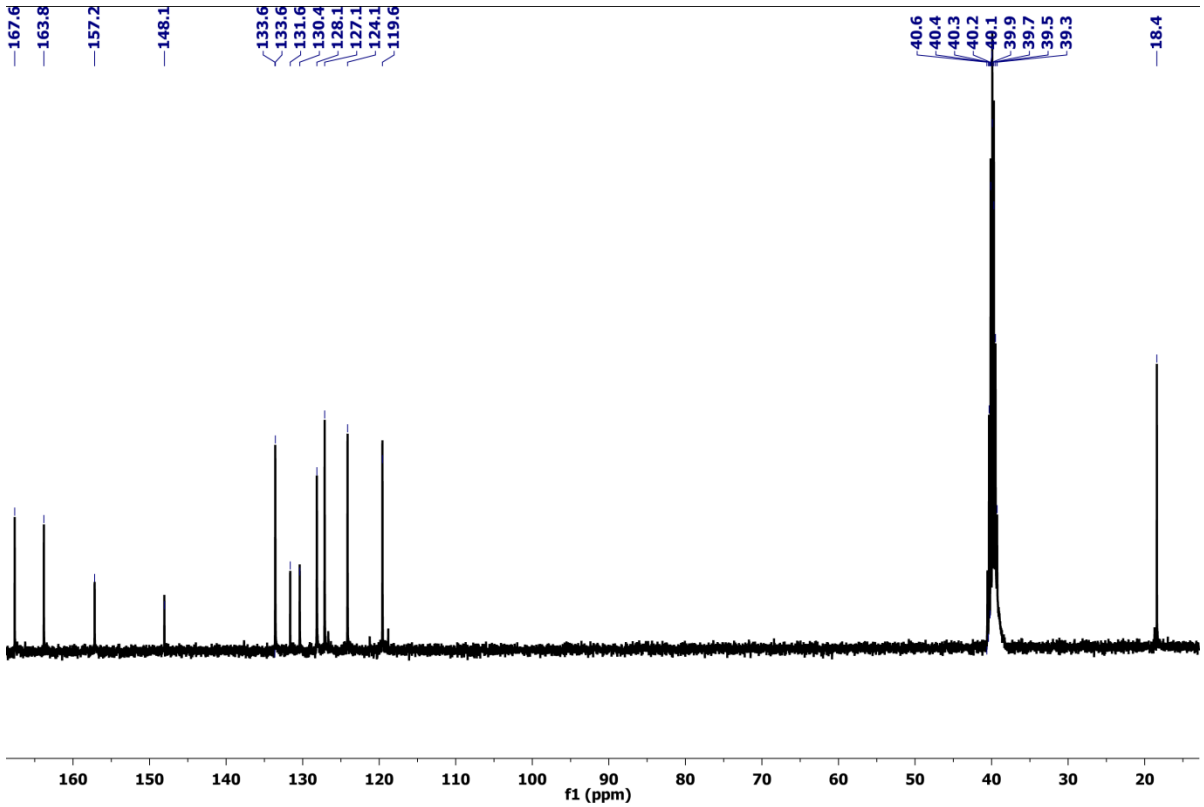

Figure S2. ^{13}C NMR spectrum of **MBA** in DMSO-d_6.

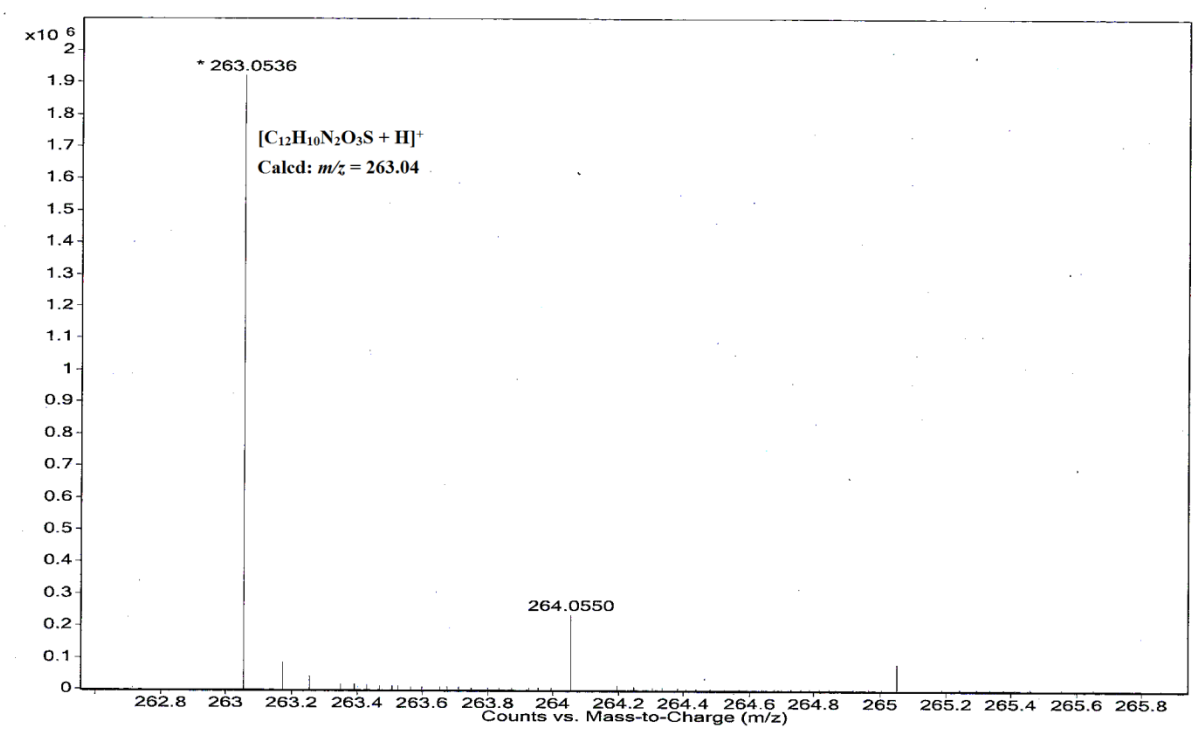

Figure S3. ESI-MS of **MBA.**

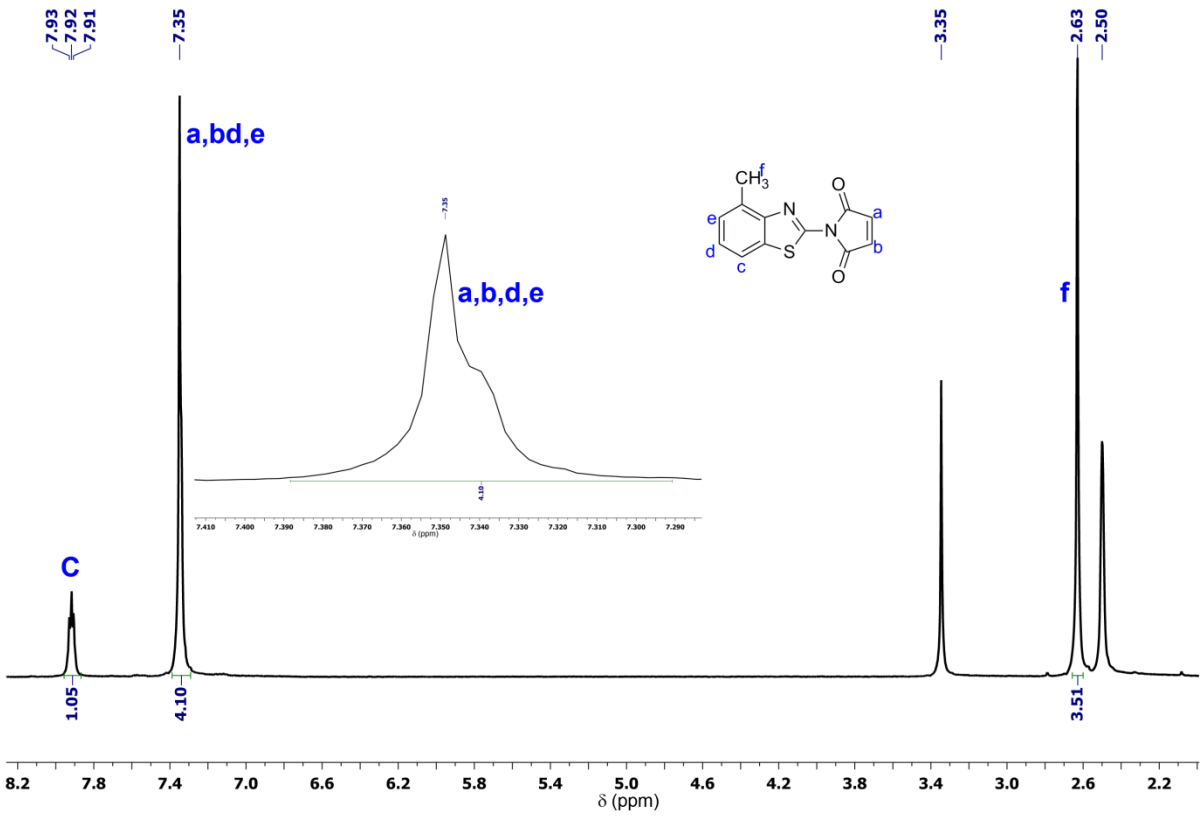

Figure S4. ^{1}H NMR spectrum of **1** in DMSO-d_6.

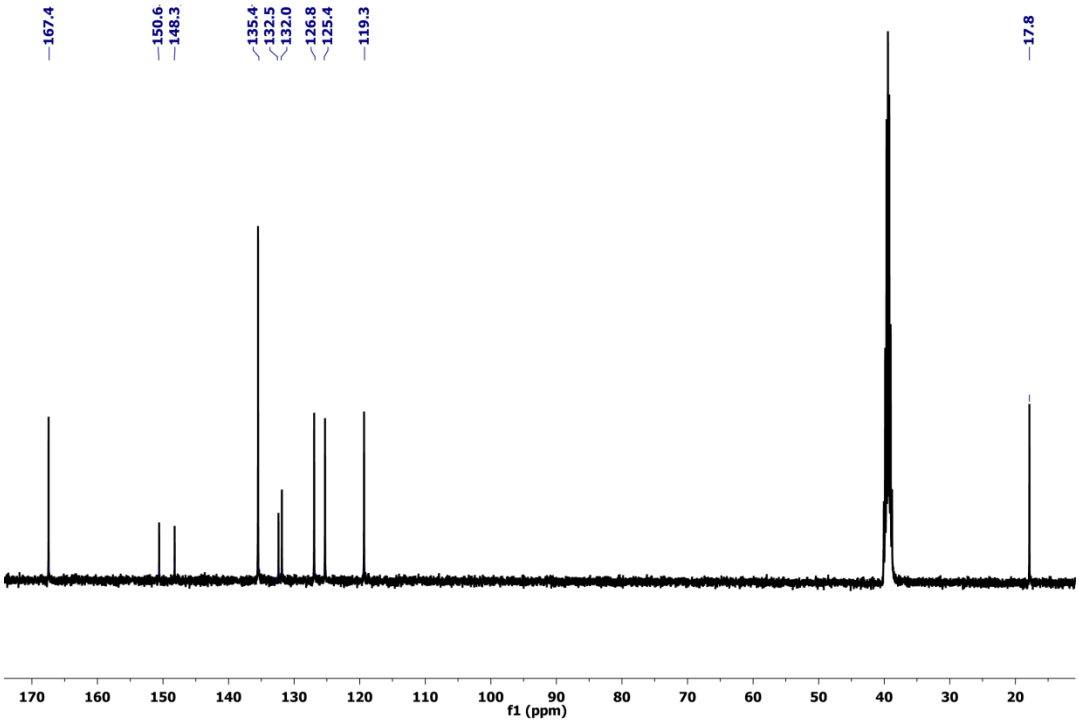

Figure S5. ^{13}C NMR spectrum of **1** in DMSO-d_6.

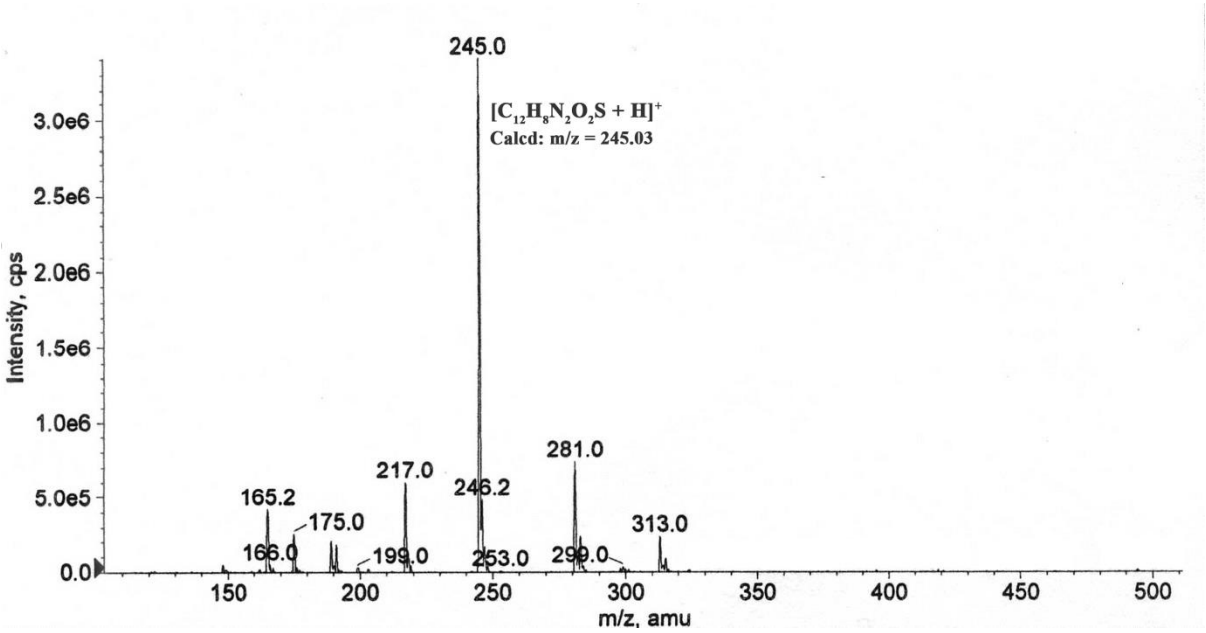

Figure S6. ESI-MS of **1.**

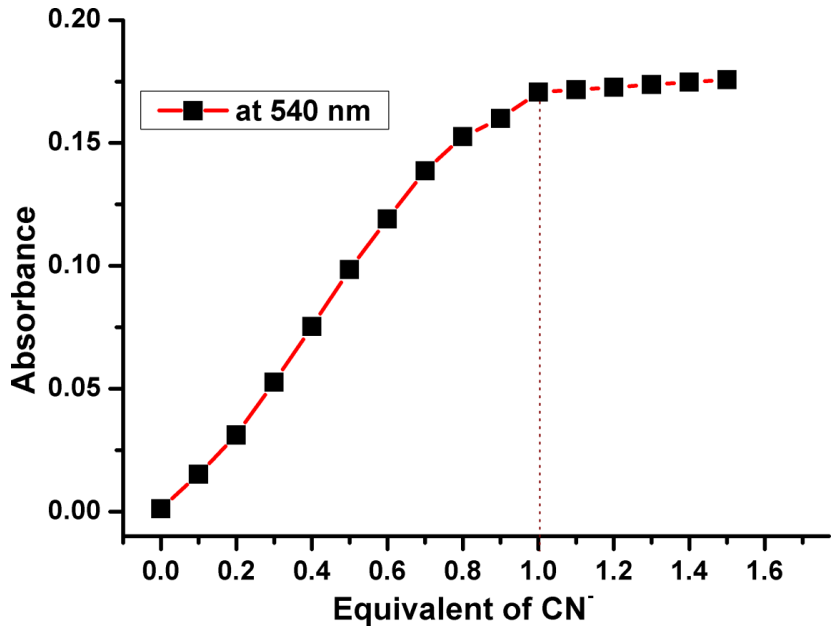

Figure S7: Changes in absorbance of **1** upon addition of TBACN (0-1.5 equiv.) in 5% aqueous DMSO at 25°C.

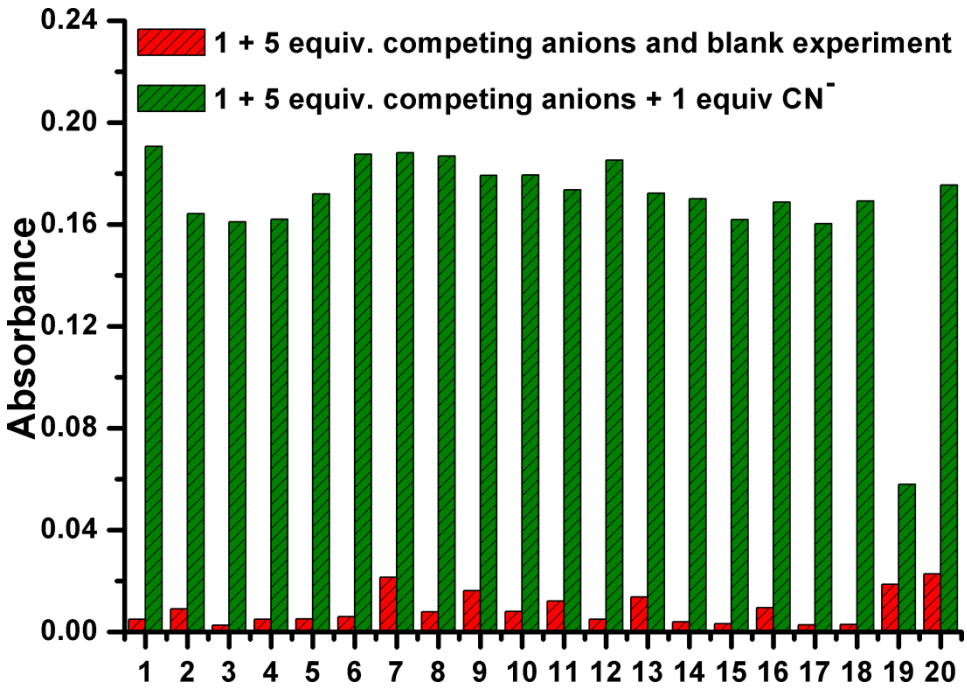

Figure S8. The UV response of **1** (100 μM) in the presence of various competing anions (5.0 equiv.) and in the absence and presence of CN^- (1 equiv.) in aqueous DMSO at 25 ºC. Where (1) Probe **1**, (2) AcO^-, (3) F^-, (4) Cl^-, (5) Br^-, (6) I^-, (7) SO_3^{2-}, (8) SO_4^{2-}, (9) $S_2O_3^{2-}$, (10) N_3^-, (11) NO_3^-,(12) ClO^-, (13) $H_2PO_4^-$, (14) HSO_4^-, (15) Histidine, (16) Serine, (17) Cysteine, (18) Gluthathione, (19) NaHS. (20) NaHS in the presence of H_2O_2 to oxidize H_2S.

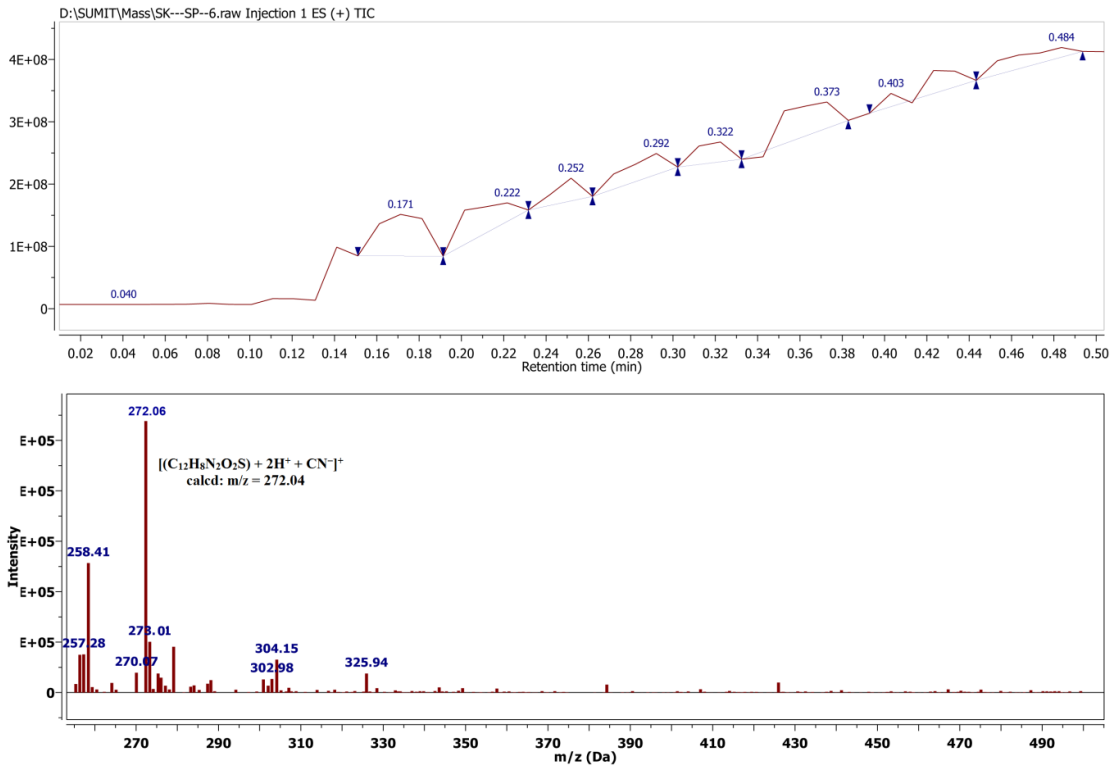

Figure S9. ESI-MS of **1** + TBACN**.**

Table S1: Main calculated optical transitions for **1,** [**1-CN**]$^-$ and **1-CN**.

Compound	Experimentally observed transition energy (eV)	Computed vertical excitation energy (eV)	Transition	Oscillator strength (*f*)
1	4.59 eV (270 nm)	4.83 eV (256 nm)	(HOMO →LUMO + 1) (HOMO →LUMO + 6)	f=0.1972
[1-CN]$^-$ (intermediate)	2.29 eV (540 nm) 3.39 eV (365 nm) 4.54 eV (273 nm)	2.31 eV (535 nm) 3.84 eV (322 nm) 4.42 eV (280 nm)	(HOMO →LUMO) (HOMO-1 → LUMO) (HOMO-2 → LUMO)	f=0.0388 f=0.0527 f=0.1039
1-CN (final)	4.53 eV (274 nm)	4.81 eV (257 nm)	(HOMO → LUMO) (HOMO-1 → LUMO)	f=0.2064

Table S2: The x,y,z Cartesian coordinates of the complex **1,** [**1-CN**]$^-$ and **1-CN**.

1				**[1-CN]$^-$**			
C	-4.13668	-0.78648	-0.0026	C	-4.6964	-0.33195	-0.20257
C	-3.03426	-1.62836	-0.00544	C	-3.69154	-1.2585	-0.46348
C	-1.77194	-1.03176	-0.00348	C	-2.3654	-0.85518	-0.30034
C	-1.61324	0.37324	0.00129	C	-2.04354	0.45274	0.11737
C	-2.73978	1.22148	0.00427	C	-3.06199	1.39006	0.38172
C	-3.98862	0.61068	0.00216	C	-4.38054	0.97074	0.21348
H	-5.13277	-1.21422	-0.00408	H	-5.73611	-0.61907	-0.32103
H	-3.15109	-2.70488	-0.00906	H	-3.93455	-2.26559	-0.78416
H	-4.87712	1.23283	0.00426	H	-5.1845	1.67359	0.41153
C	-2.57168	2.71666	0.00978	C	-2.70793	2.78393	0.82726
H	-3.54176	3.21674	0.00832	H	-3.60784	3.38026	0.9996
H	-2.0122	3.04455	0.89012	H	-2.11628	2.7632	1.7469
H	-2.00625	3.05047	-0.86445	H	-2.08835	3.28892	0.0804
N	-0.3025	0.81747	0.00285	N	-0.6959	0.72164	0.2398
C	0.51665	-0.17397	-0.00055	C	0.02347	-0.31551	-0.06328
S	-0.19545	-1.78923	-0.00619	S	-0.89537	-1.78793	-0.54894
N	1.91595	-0.02644	-0.00031	N	1.39641	-0.35088	-0.03697
C	2.70752	0.13124	1.16254	C	2.23978	0.43549	-0.80993
C	2.70659	0.14457	-1.16193	C	2.19362	-1.31244	0.84394
C	4.09699	0.39995	-0.66507	C	3.51627	-1.08047	0.56972
H	4.91867	0.55537	-1.34899	H	4.32796	-1.60162	1.05025
C	4.09752	0.39232	0.66757	O	1.95392	1.2815	-1.62271
H	4.91974	0.53992	1.35256	O	1.55335	-2.07558	1.57982
O	2.31973	0.05893	2.29796	C	3.68913	-0.00802	-0.46182
O	2.31795	0.08511	-2.29779	H	4.12855	-0.34992	-1.41296
				C	4.50011	1.14017	-0.03198
				N	5.18358	2.00402	0.31649

1-CN			
C	-4.63477	-0.83059	0.40105
C	-3.5161	-1.65056	0.37684
C	-2.27754	-1.03666	0.18355
C	-2.158	0.36191	0.01572
C	-3.30037	1.18791	0.04207
C	-4.52551	0.56041	0.23674
H	-5.61359	-1.27175	0.55027
H	-3.60364	-2.72222	0.50407
H	-5.42589	1.16446	0.26287
C	-3.1734	2.67663	-0.13382
H	-4.15173	3.15808	-0.09008
H	-2.53784	3.10986	0.64326
H	-2.7088	2.91986	-1.0932
N	-0.86531	0.82167	-0.17169
C	-0.03089	-0.15473	-0.15046
S	-0.68891	-1.76758	0.10302
N	1.36486	0.02726	-0.3079
C	2.19685	0.42994	0.74754
O	1.87625	0.55859	1.89235
O	1.49261	-0.39125	-2.58456
C	3.58891	0.71397	0.13152
H	3.70121	1.80342	0.15274
C	4.67246	0.13349	0.91382
N	5.54671	-0.33649	1.49917
C	3.49797	0.20049	-1.32125
H	3.84988	0.92094	-2.05915
H	4.05795	-0.72561	-1.46638
C	2.02378	-0.09248	-1.552

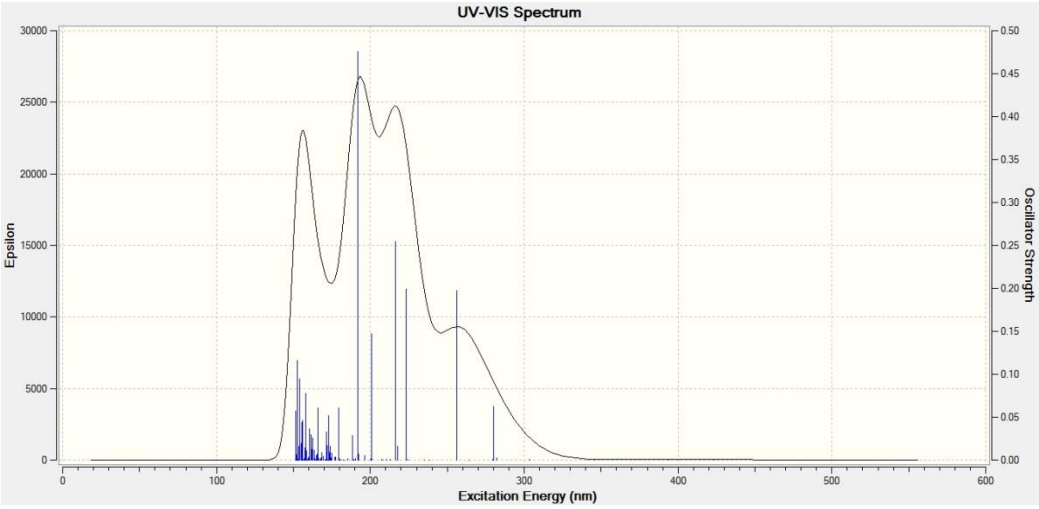

(a)

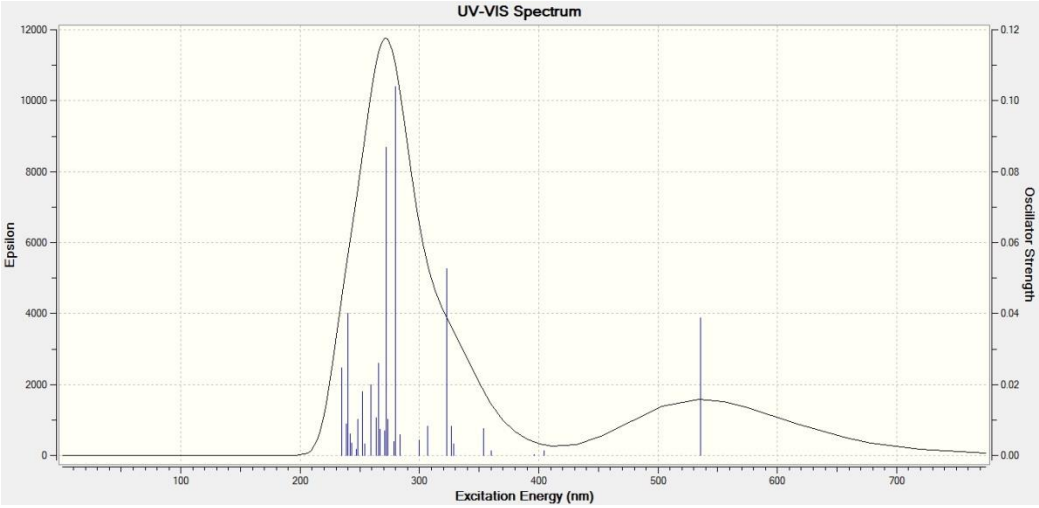

(b)

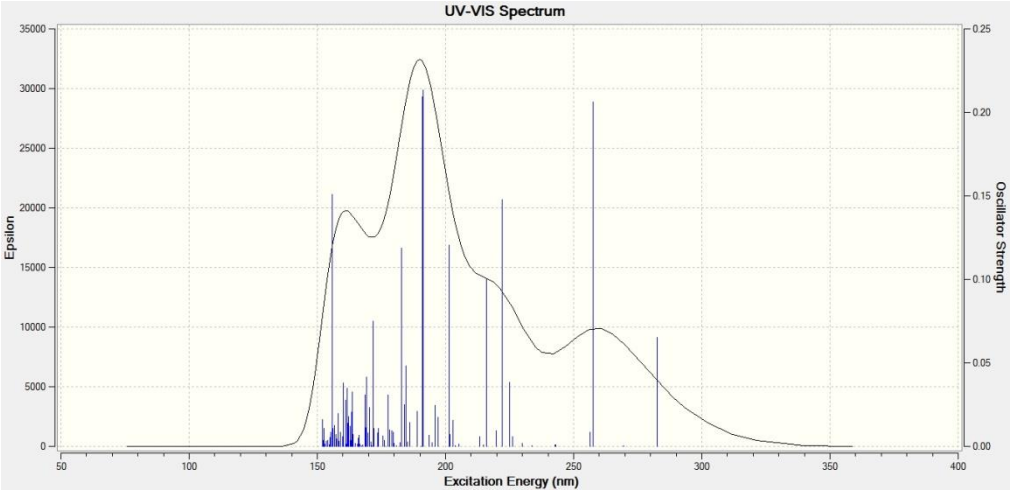

(c)

Figure S10. Theoretical UV-vis spectrum of (a) probe **1,** (b) [**1-CN**]$^-$ and (c) **1-CN**.

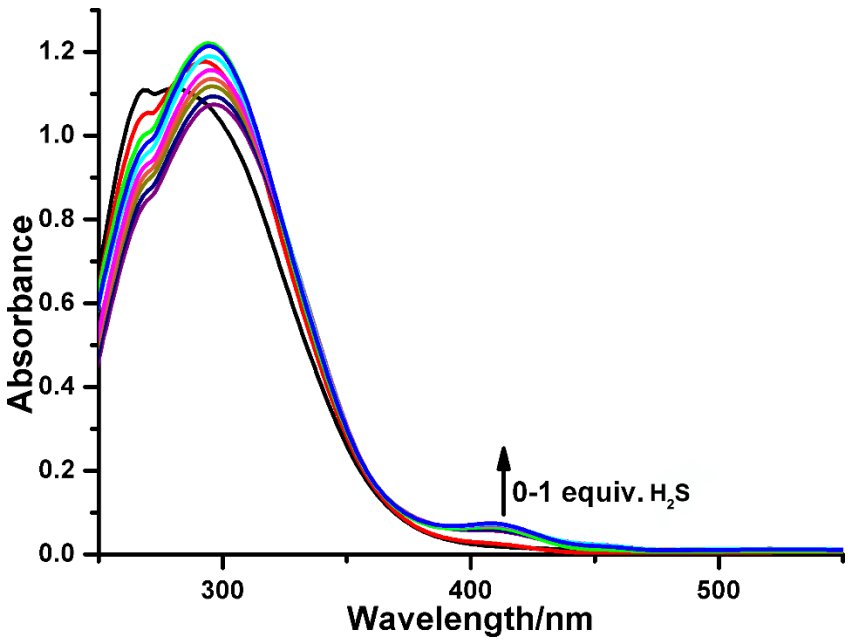

Figure S11. UV−vis absorption titration of **1** (100 μM) with H_2S (0−1.0 equiv.) in DMSO /Tris-HCl buffer (v/v, 1:1; pH 7.0) at 25 °C.

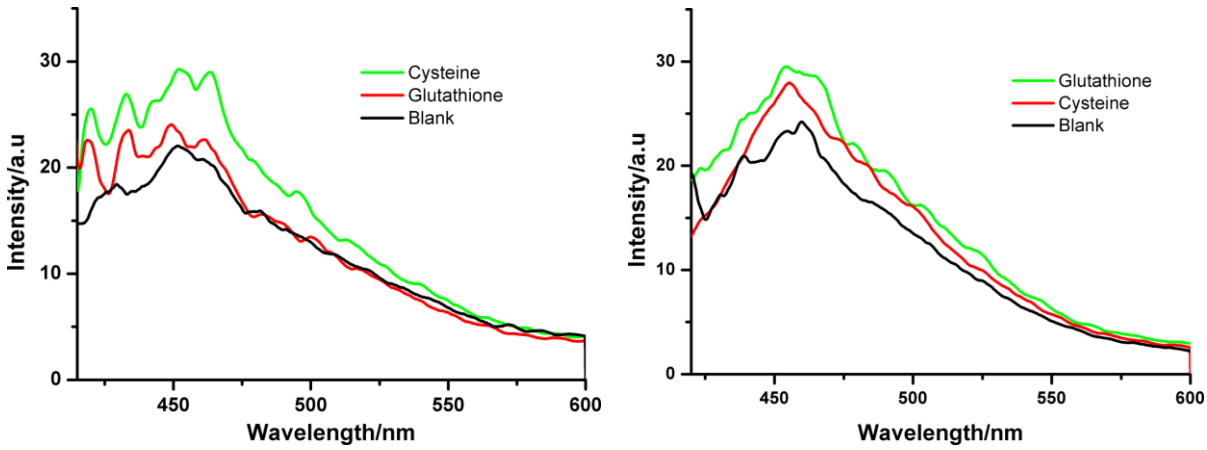

(a) (b)

Figure S12. The fluorescence response of probe **1** (100 μM) with 2.0 equiv. of cysteine and glutathione in DMSO /Tris-HCl buffer (v/v, 1:1) at (a) pH 8.2 (b) pH 9.2.

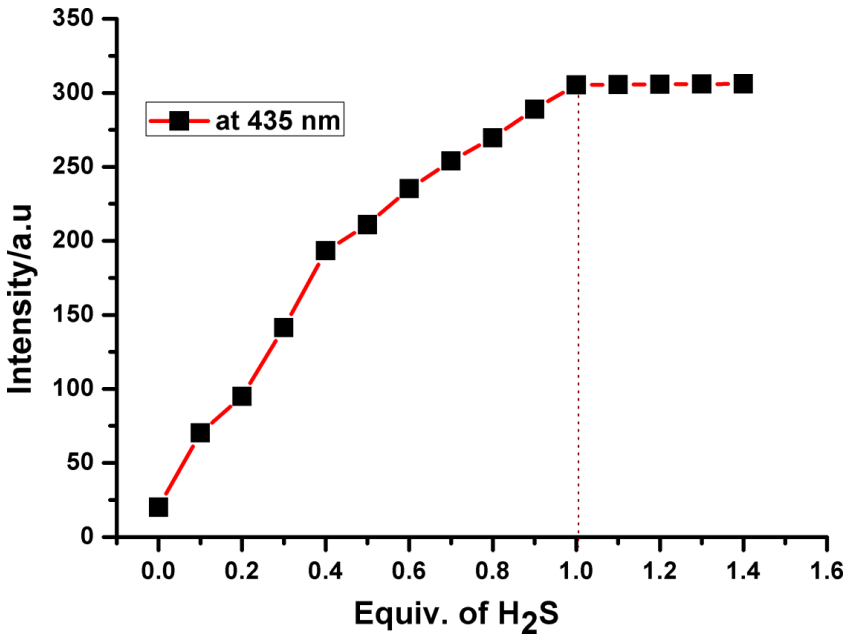

Figure S13. Changes in fluorescence intensity of **1** upon addition of H_2S (0-1.4 equiv.) in DMSO /Tris-HCl buffer (v/v, 1:1; pH 7.0) at 25°C.

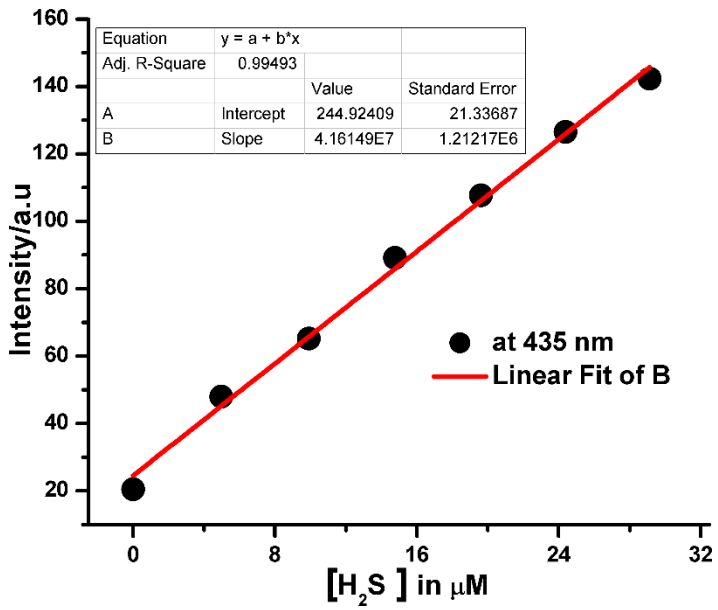

Figure S14. A calibration curve for H_2S over a concentration range between 0 - 30 μM derived from fluorescence titration with **1**(100.0 μM). The detection limits were calculated according to the equation DL = 3 × SD/slope. SD corresponds to the standard deviation of the blank sample (obtained by the 10 consecutive scan of the blank sample.

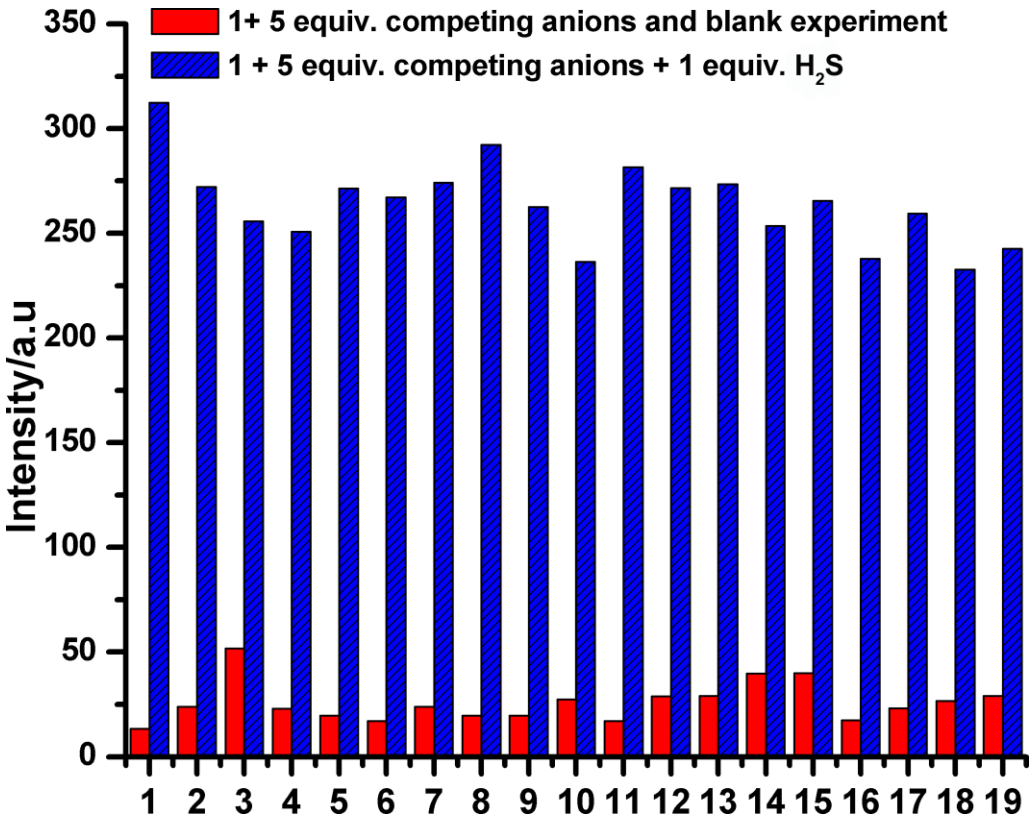

Figure S15. The fluorescence response of **1** (100 μM) in presence of various competing anions (5 equiv.) and in the absence and presence of H_2S (1 equiv.) in DMSO/buffer (1:1; v/v; pH 7.0) at 25 ºC. Fluorescence (λ_{ex} = 410 nm) was monitored at λ_{em} = 435 nm.(1) Blank, (2) CN^- , (3) AcO^-, (4) F^-, (5) Cl^-, (6) Br^-, (7) I^-, (8) SO_3^{2-}, (9) SO_4^{2-}, (10) $S_2O_3^{2-}$, (11) N_3^-, (12) NO_3^-,(13) ClO^-, (14) $H_2PO_4^-$, (15) HSO_4^-, (16) Histidine, (17) Serine, (18) Cysteine, (19) Gluthathione.

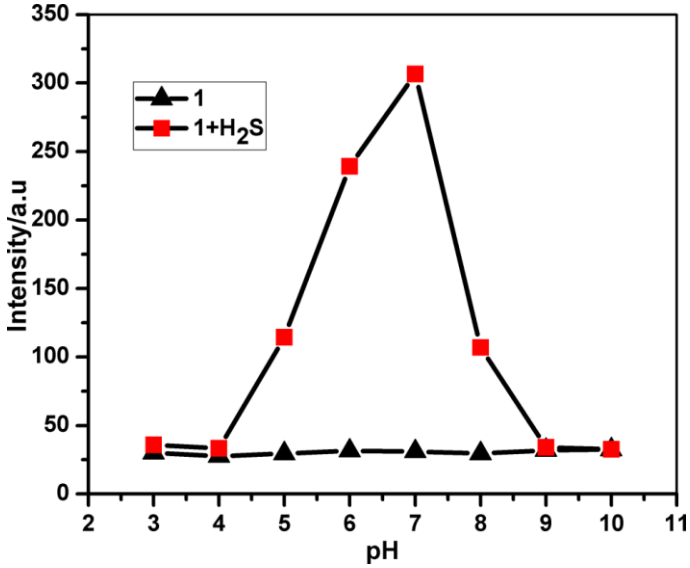

Figure S16. The effect of pH on the fluorescence response of **1** (100 μM) with H_2S (1.0 equiv.) (λ_{ex} = 410 nm) in DMSO /Tris-HCl buffer (1:1; v/v) at 25 ºC (λ_{em} = 435 nm).

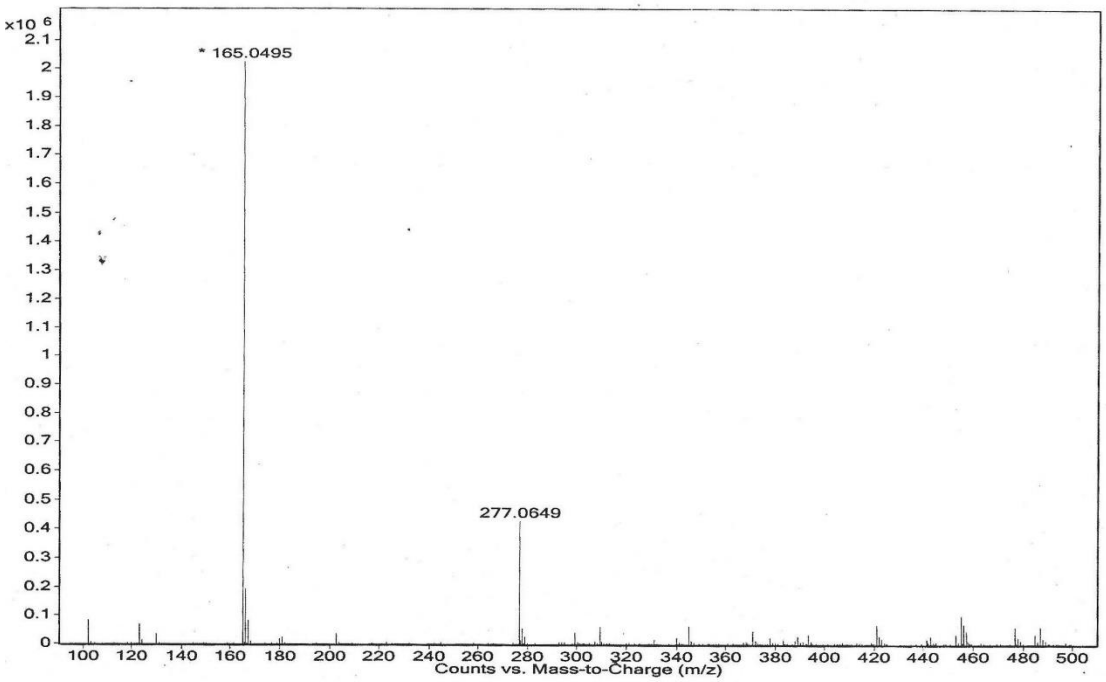

Figure S17. ESI-MS of **1-SH** adduct.

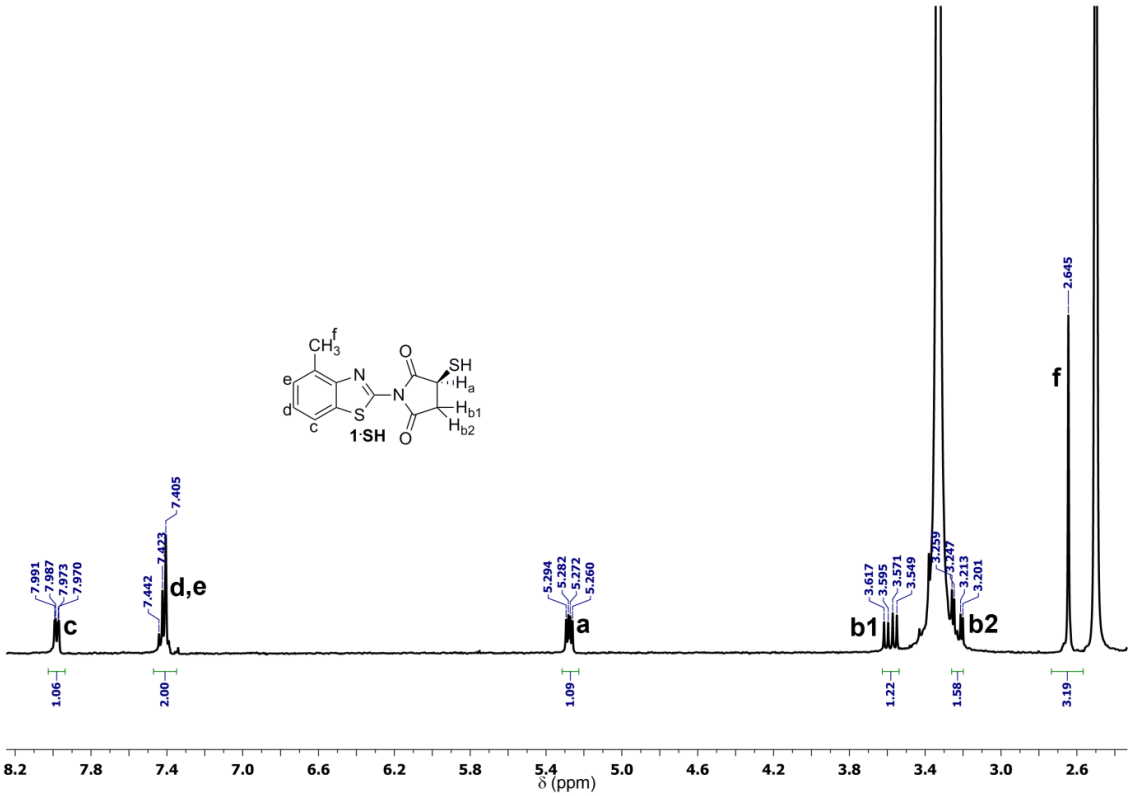

Figure S18. ^{1}H NMR spectrum of **1-SH** adduct in DMSO-d_6.

HPLC Analysis:

Enantiomeric purity (100%) was determined by chiral HPLC analysis on DIACEL CHIRALPAK OD-H column, acetonitrile (100%), retention times: t_R = 7.239 min, flow 0.5 ml/min, UV 254 nm.

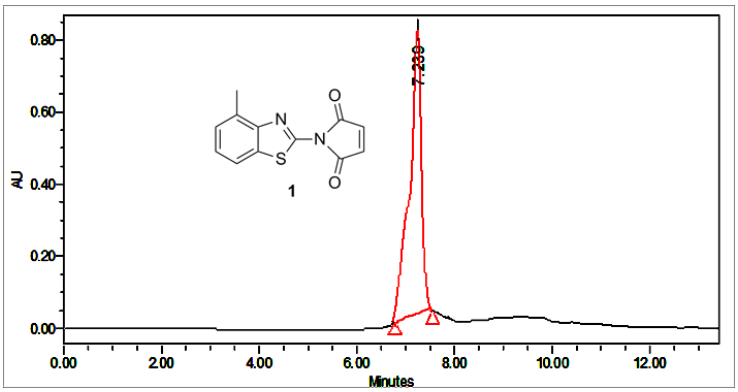

	Name	Retention Time	Area	% Area	Height
1		7.239	12979466	100.00	785325

(a)

Enantiomeric ratio (49.33: 50.67) was determined by chiral HPLC analysis on DIACEL CHIRALPAK OD-H column, acetonitrile (100%), retention times: t_{R1} =8.646 min, t_{R2} =9.590 min, flow 0.5 ml/min, UV 254 nm.

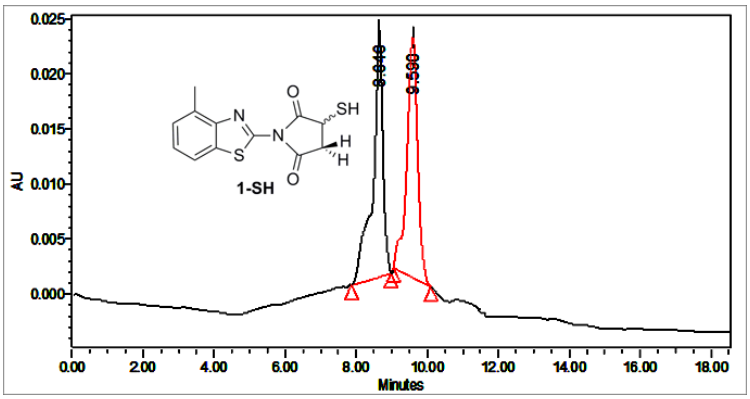

	Name	Retention Time	Area	% Area	Height
1		8.646	449555	49.33	22486
2		9.590	461777	50.67	21839

(b)

Figure S19. HPLC analysis of (a) probe **1**, (b) **1-SH.**

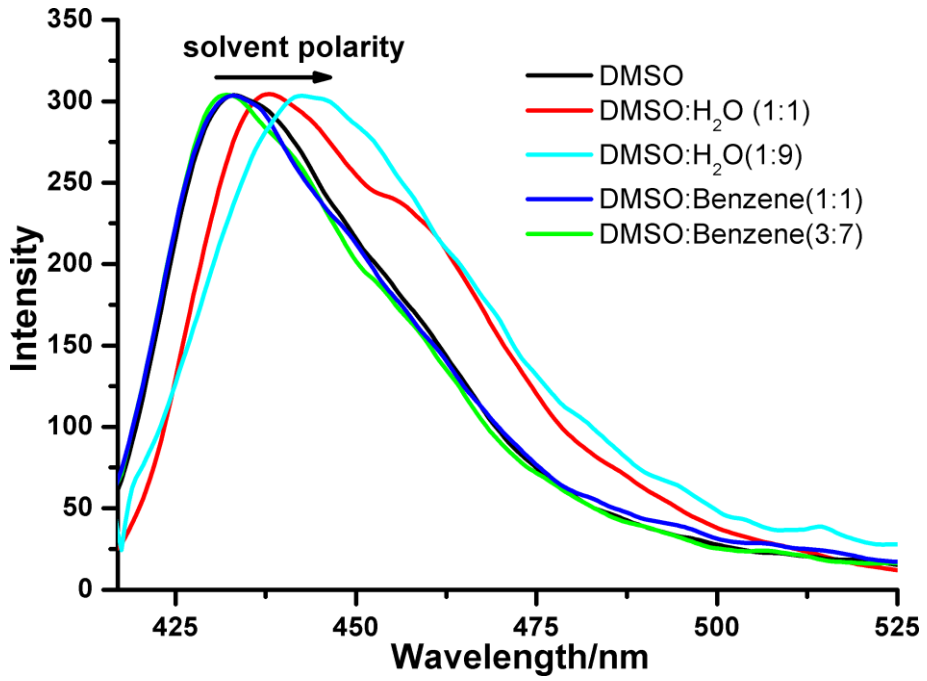

Figure S20. The fluorescence response of **1-SH** in solvents with different polarities.

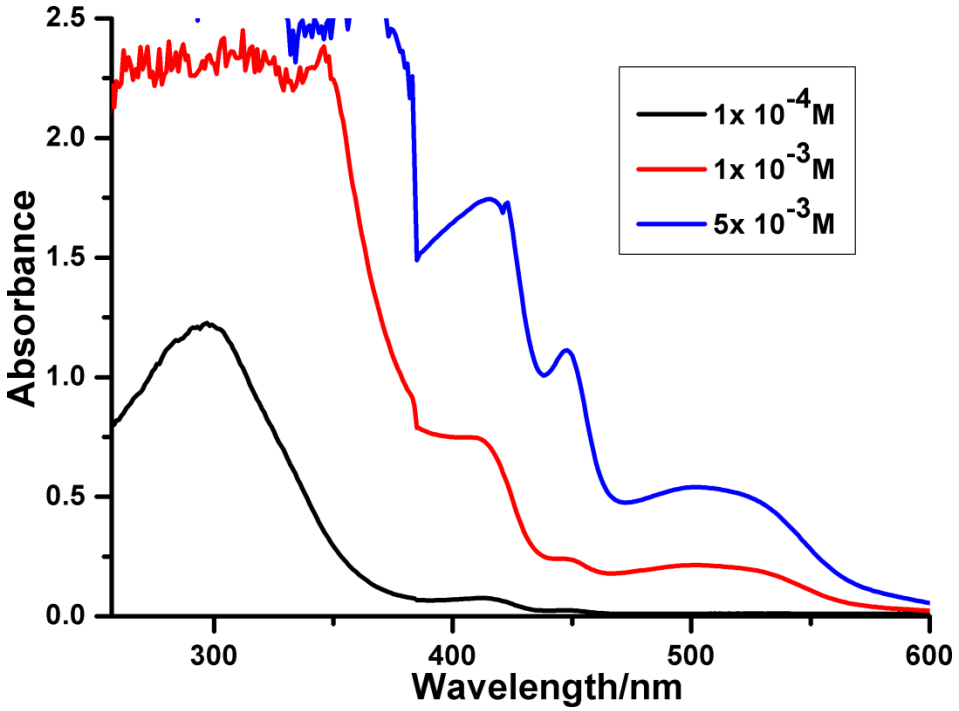

Figure S21. UV−vis absorption of **1-SH** adduct in DMSO /Tris-HCl buffer (v/v, 1:1; pH 7.0) in different concentration at 25 °C.

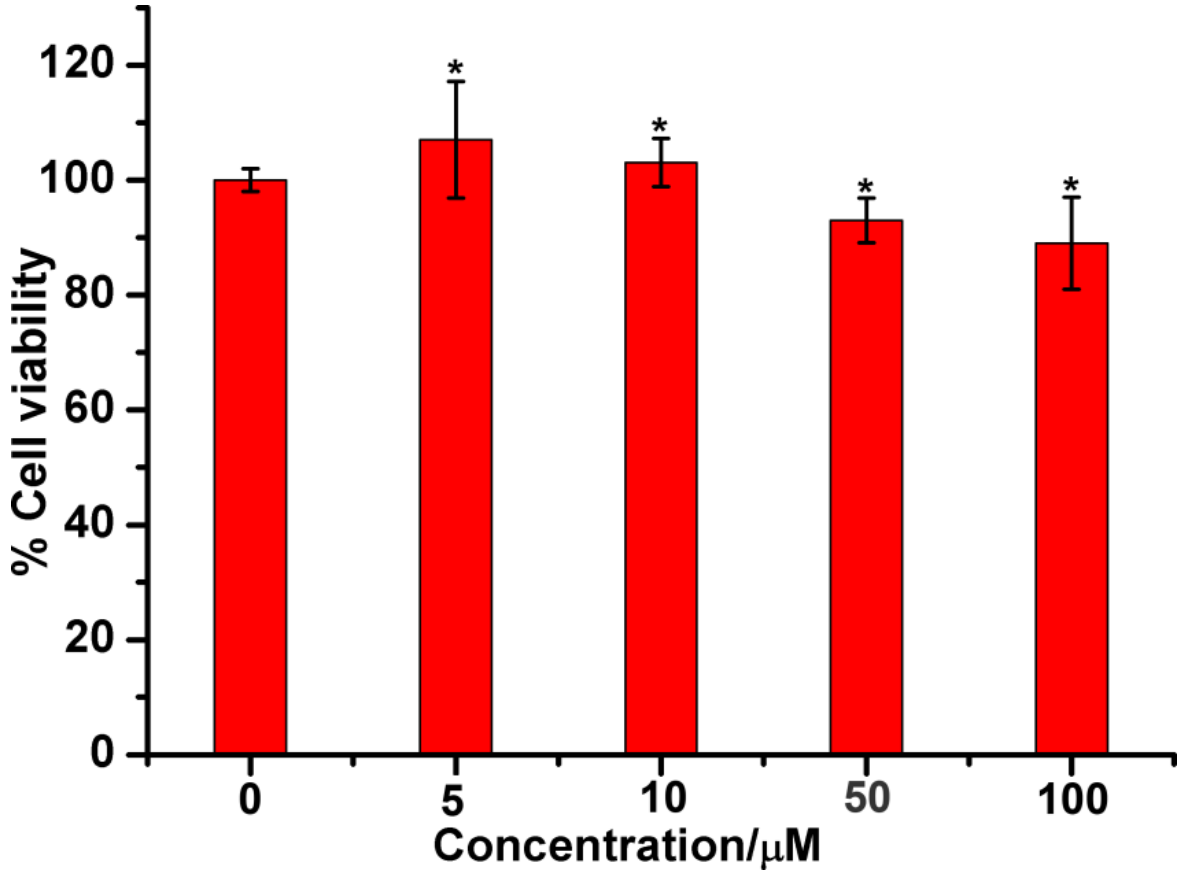

Figure S22: Cell viability of HeLa cells in the presence of different concentrations of **1** for 24 h. Data is expressed as the mean value for four separate trials. Asterisks(*) denote significantly different from the control (0 μM of **1**) at $p \leq 0.05$.

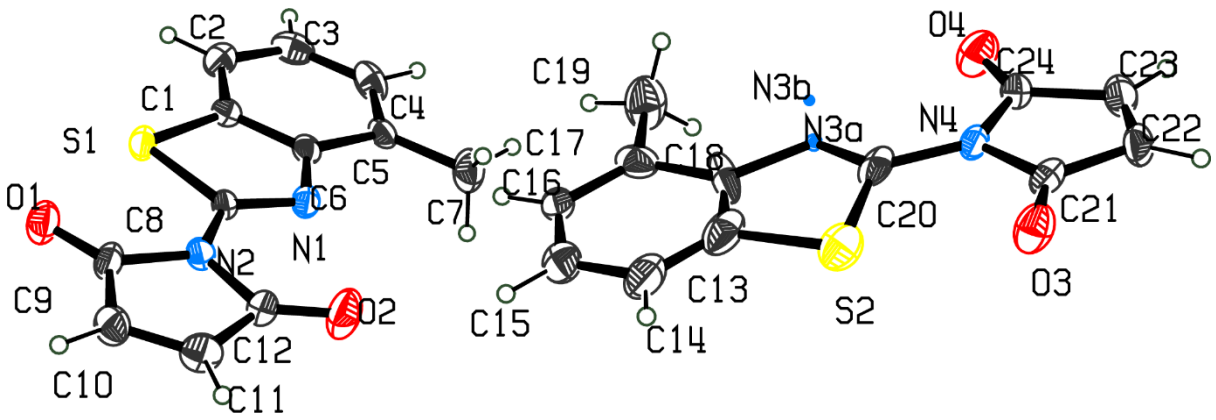

Figure S23. ORTEP plot of probe **1** with 30% thermal ellipsoids probability

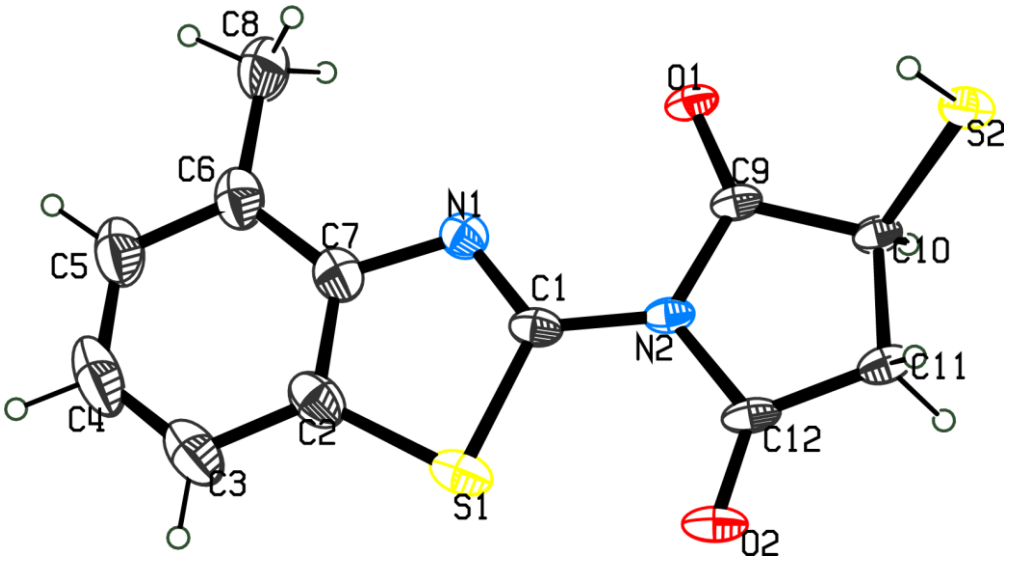

Figure S24. ORTEP plot of **1-SH** adduct with 30% thermal ellipsoids probability.

Table S3. Crystal data and structure refinement for **1** and **1-SH.**

	1	**1-SH**
Empirical formula	$C_{24}H_{16}N_4O_4S_2$	$C_{12}H_{10}N_2O_2S_2$
Formula weight	488.53	278.34
Temperature	293(2) K	293(2) K
Wavelength	0.71073 Å	0.71073 Å
Crystal system	Triclinic	Orthorhombic
Space group	*P*-1	*P*ca2$_1$
Unit cell dimensions	a = 7.1678(9) Å	a = 10.8100(8) Å
	b = 10.6157(14) Å	b = 14.1314(16) Å
	c = 14.7091(19) Å	c = 8.1358(6) Å
	α = 84.423(11)$^\circ$	α = 90°.
	β = 85.186(11)$^\circ$	β = 90°.
	γ = 77.350(11)$^\circ$	γ = 90°.
Volume, Z	1084.6(2) Å^3, 2	1242.83(19) Å^3, 4
Density (calcd.)	1.496 Mg/m^3	1.488 Mg/m^3
Absorption coefficient	0.287 mm^{-1}	0.422 mm^{-1}
F(000)	504	576
Θ range for data collection	3.153 to 26.965°.	3.450 to 29.049°
Reflections collected	5457	3280
Independent reflections	3947 [*R(int)* = 0.0300]	2108 [*R(int)* = 0.0152]
Refinement method	Full-matrix least-squares on F^2	Full-matrix least-squares on F^2
Data / restraints / parameters	3947 / 0 / 309	2108 / 1 / 165
Goodness-of-fit on F^2	1.092	1.067
Final *R* indices [$I>2\sigma(I)$]	$R1$ = 0.1073, $wR2$ = 0.2901	$R1$ = 0.0325, $wR2$ = 0.0865
R indices (all data)	$R1$ = 0.1410, $wR2$ = 0.3233	$R1$ = 0.0375, $wR2$ = 0.0909
Largest diff. peak and hole	1.566 and -0.615e.Å^{-3}	0.245 and -0.225 e.Å^{-3}
Flack(x) parameter	-	-0.06(4)

##END##